

Finite temperature properties of alternating ferro-antiferromagnetic Heisenberg chains

Niklas Casper^{1,*} and Wolfram Brenig^{1,†}

¹*Institute for Theoretical Physics, Technical University Braunschweig, D-38106 Braunschweig, Germany*

(Dated: January 15, 2020)

We present a study of the spin-1/2 Heisenberg chain with alternating ferro- and antiferromagnetic exchange, focusing on the role of the exchange couplings to cover both, dimer and Haldane limit. Employing a complementary combination of perturbation theory and quantum Monte Carlo simulation, we report results for the magnetic susceptibility as well as the dynamic structure factor over a wide range of coupling constants and for different temperatures to extract the spin gap. For a small ferromagnetic coupling, we find good agreement between perturbation theory and quantum Monte Carlo. For arbitrary exchange couplings we show that the dynamic structure factor, obtained from quantum Monte Carlo, scales between triplons and a Haldane chain spectrum. Finally, we contrast our findings for the spin gap versus the exchange couplings against existing literature.

I. INTRODUCTION

Homogeneous nearest-neighbor (NN) spin- S antiferromagnetic chains (AFC) exist in two variants. Namely gapless for $S = (2N + 1)/2$, versus gapped for $S = N$, as conjectured by Haldane [1]. Apart from a non-degenerate singlet ground for both variants and apart from an expected difference in their correlation functions, i.e. algebraic versus exponential, induced by the presence or absence of the spin gap, $S=1$ Haldane-chains are fundamentally different from $S=1/2$ AFCs, since the former exhibit a finite string order parameter (SOP) [2, 3]. This translates into a symmetry protected topological ground state of the Haldane chain, and the existence of edge-modes in open boundary systems, which arise naturally in the AKLT representation of the ground state [4].

Early on *inhomogeneous* $S=1/2$ chains have been investigated for their potential similarities to Haldane chains. In particular bond-alternating $S=1/2$ antiferro- and ferro-antiferromagnetic chains (AAC and FAC) have been under intense scrutiny. First exact diagonalization (ED) studies of the specific heat and the magnetic susceptibility of the FAC have performed in Ref. [5]. Extensive analysis of the quantum phase diagram of the AAC and FAC by density matrix renormalization group (DMRG) has shown almost all of the parameter space to represent Haldane chain behavior [6], consistent with bosonization and ED calculations of the SOP [7] and findings regarding universality at the magnetic field induced transition into a Luttinger liquid in the FAC [8]. Excitation spectra and dynamic structure factor calculations for the FAC have been performed at zero temperature, $T=0$, by ED on finite systems up to 26 sites [6, 9, 10] and by bond operator mean field theory [10, 11]. Finite temperature studies of the specific heat, susceptibility and magnetization of the FAC have

also been performed using quantum Monte-Carlo (QMC) [12, 13] including analysis of the spin gap with [13] and without [12] inter-chain coupling.

Significant efforts have been made to synthesize spin-1/2 FACs. In early materials attempts [14, 15], quasi one-dimensional (1D) behavior was masked by interchain exchange, inducing magnetic long-range order (LRO) at rather high temperatures. Subsequent analysis however of the compounds CuNb_2O_6 [16, 18], DMACuCl_3 [17, 19, 20], $\text{Na}_3\text{Cu}_2\text{SbO}_6$ [21–23], the zinc-verdazyl complex $\text{C}_{29}\text{H}_{18}\text{F}_{12}\text{N}_5\text{O}_4\text{Zn}$ [13], and $\text{BaCu}_2\text{V}_2\text{O}_8$ [24] by thermodynamics, including magnetization and magnetic susceptibility measurements, as well as nuclear magnetic resonance and inelastic neutron scattering provided clear evidence of FAC and possibly also Haldane chain behavior.

Despite these extensive efforts, many open questions still remain to be investigated for the FAC. From a theoretical point of view this applies in particular to the *finite temperature* spin-dynamics. Therefore, in this work, we will advance QMC calculations of the momentum resolved dynamic structure factor $S(k, \omega)$ at $T \neq 0$. Moreover, its features, and in particular the spin gap will be contrasted against calculations using perturbation theory and static QMC. The paper is organized as follows. In Sec. II we describe the model. Sec. III comprises a short summary of the quantum Monte Carlo method we use. Following this, in Sec. IV, we detail our results, including the thermodynamic susceptibility, the dynamic structure factor, and the evolution of the spin gap. We conclude and summarize our findings in Sec. V.

II. MODEL

The Hamiltonian of the spin-1/2 FAC reads

$$H = \sum_{i=0}^{N/2} (J_F \mathbf{S}_{2i} \cdot \mathbf{S}_{2i+1} + J_{AF} \mathbf{S}_{2i+1} \cdot \mathbf{S}_{2i+2}) - h \sum_{i=0}^{N-1} S_i^z. \quad (1)$$

*Electronic address: n.casper@tu-bs.de

†Electronic address: w.brenig@tu-bs.de

	$S = 1$	$S = 1/2$
singlet E_0	$-2J_{\text{AF}}$	$-1/4(1 - 2j + 2\sqrt{1 + 2j + 4j^2})$
triplet E_1	$-J_{\text{AF}}$	$-1/4(1 + 2\sqrt{1 + j^2})$
gap $\Delta = E_1 - E_0$	J_{AF}	$\lim_{j \rightarrow \infty} \Delta = J_{\text{AF}}/4$

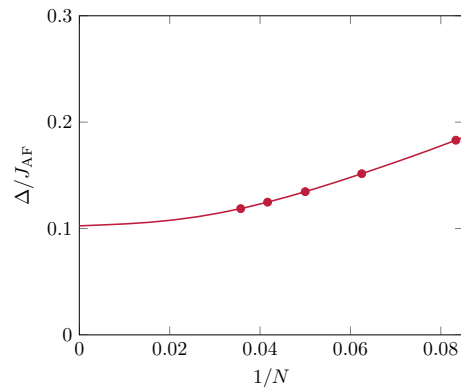
TABLE I: Spectra of $S=1$ dimer and $N=4$, $S=1/2$ FAC

$\mathbf{S}_i = (S_i^x, S_i^y, S_i^z)$ are $S=1/2$ operators at sites i of a chain with $N/2$ unit cells with periodic boundary conditions (PBC). The ferro- and antiferromagnetic exchange couplings are labeled by $J_{\text{F}} < 0$ and $J_{\text{AF}} > 0$, with a dimensionless parameter $j = |J_{\text{F}}/J_{\text{AF}}|$ used hereafter. h refers to an external magnetic field. With $N = 4\mathbb{N}$ spins, the system is frustration-free.

In the limiting case of $j = 0$, the chain consists of $N/2$ decoupled antiferromagnetic dimers with a singly degenerate singlet-product ground state and an energy gap of $\Delta = J_{\text{AF}}$ to a $3N/2$ -fold degenerate set of first excited triplet states. For $j \neq 0$, but still $j \ll 1$ the latter set splits into a gas of dispersive and interacting triplon excitations. In the opposite limit, i.e. $1/j = 0$ the system comprises $N/2$ decoupled ferromagnetic dimers in triplet states with a $3^{N/2}$ -fold ground state degeneracy and an energy gap of $\Delta = J_{\text{F}}$ to an $N/2$ -fold degenerate set of first excited singlet states. For $1/j \neq 0$, but still $1/j \ll 1$ the ground state degeneracy is lifted and the triplets are coupled into an effective low-energy antiferromagnetic spin-1 chain, i.e. the Haldane chain [1].

Starting with early ED-work [25], more recent analysis using QMC [26] and DMRG [27] has converged to a spin gap of $\Delta_H/J \simeq 0.41050(2)$ for the Haldane chain, where J is the exchange coupling constant. It is tempting to identify the latter J with J_{AF} of the FAC in the asymptotic situation $1/j \rightarrow 0$, but $J_{\text{AF}} \neq 0$, and therefore to also expect a gap of $\Delta/J_{\text{AF}} \simeq 0.41$ for the FAC [12]. However, since bond-correlation functions on the AF bonds in the FAC, i.e. $\langle \mathbf{S}_{2i-1} \cdot \mathbf{S}_{2i} \rangle$ are reduced by a factor of 4 as compared to the bond-correlation functions of a fictitious Haldane chain [28] with spin $L = 1$, i.e. $\langle \mathbf{L}_i \cdot \mathbf{L}_{i+1} \rangle = 4 \langle \mathbf{S}_{2i} \cdot \mathbf{S}_{2i+1} \rangle$, one instead should expect a rescaling of the spin gap by a factor of $1/4$.

We emphasize the previous point in two ways. First, in Table I we compare the spectra of two toy models, namely an $L = 1$ AF dimer and a FAC chain of length $N = 4$, both with open boundary conditions. By defining the gap as the difference of energies between the lowest triplet and singlet states, an exact reduction of the gap by $1/4$ is obvious. Second, in Fig. 1 we show a polynomial fits in $1/N$ to small system diagonalization using Lanczos from the ALPS project [29]. Already for these very short chains ($N = 12 \dots 28$) an extrapolated value of $\Delta/J_{\text{AF}} \approx 0.1025 = 0.41/4$ is manifest.

FIG. 1: Finite size scaling of spin gap (solid dots) from Lanczos [29] for $N = 12 \dots 28$. Solid line is a non-linear fit.

III. QUANTUM MONTE CARLO METHOD

The numerical results obtained in this work are based on QMC calculations using the stochastic series expansion (SSE), as pioneered in Refs. [30–32]. This method is based on an importance sampling of the high temperature series expansion of the partition function

$$Z = \sum_{\alpha} \sum_{S_M} \frac{(-\beta)^n (M-n)!}{M!} \left\langle \alpha \left| \prod_{p=1}^M H_{a_p, b_p} \right| \alpha \right\rangle, \quad (2)$$

where $\beta = 1/T$ is the inverse temperature, $H_{1,b} = C - S_{b1}^z S_{b2}^z$ and $H_{2,b} = (S_{b1}^+ S_{b2}^- + S_{b1}^- S_{b2}^+)/2$ are the spin diagonal and off-diagonal bond operators, and M the truncation order. C must be chosen such that all diagonal weights are nonnegative. $|\alpha\rangle = |S_1^z, \dots, S_N^z\rangle$ refers to the S^z basis and $S_M = [a_1, b_1][a_2, b_2] \dots [a_M, b_M]$ is an index for the so-called operator string $\prod_{p=1}^M H_{a_p, b_p}$. This string is Metropolis sampled, using two types of updates, i.e. diagonal updates which change the number of diagonal operators H_{1,b_p} in the operator string and loop updates which change the type of operators $H_{1,b_p} \leftrightarrow H_{2,b_p}$. For bipartite lattices the loop update comprises an even number of off-diagonal operators H_{2,b_p} , ensuring positivity of the transition probabilities. The order M of the expansion is truncated depending on T , such as to have no impact on precision.

The dynamic structure factor can be obtained from QMC in real space by a conversion of the discrete expansions slices to continuous imaginary time via a binomial distribution [30]

$$\langle S_i(\tau) S_j(0) \rangle = \left\langle \sum_{m=0}^M \binom{M}{m} \left(\frac{\tau}{\beta} \right)^m \left(1 - \frac{\tau}{\beta} \right)^{M-m} \frac{1}{M} \sum_{p=0}^{M-1} S_i^+(m+p) S_j^-(p) \right\rangle_W, \quad (3)$$

where i, j refer to sites, and τ to the imaginary time. $m + p, p$ on the right hand side label positions within the operator string, and $\langle \dots \rangle_W$ denotes the Metropolis weight of an operator string of length M generated by the SSE [31, 32]. From Eq. (3) one can proceed to momentum space by Fourier transformation

$$S(k, \tau) = \sum_i e^{ikr_i} \langle S_i(\tau) S_0(0) \rangle / N. \quad (4)$$

Since the model comprises two sites per unit cell we evaluate an even(odd) structure factor $S_{\text{even(odd)}}(k, \omega)$ by summing over $i=2l(i=2l+1)$ in Eq. (4) including the on-site/bond correlators. Finally, the dynamic structure factor in frequency and momentum space is obtained from analytic continuation, which is equivalent to an inversion for $S(k, \omega)$ of

$$S(k, \tau) = \int_0^\infty d\omega S(k, \omega) K(\omega, \tau), \quad (5)$$

with a kernel $K(\omega, \tau) = (e^{-\tau\omega} + e^{-(\beta-\tau)\omega})/\pi$.

The preceding inversion is an ill-posed problem, for which maximum entropy methods (MEM) have proven to be well suited. We have used Bryan's MEM algorithm [33, 34]. This method minimizes the functional $Q = \chi^2/2 - \alpha\sigma$, with χ being the covariance of the QMC data with respect to the MEM trial spectrum $S(k, \omega)$. Overfitting is prevented by an entropy term $\sigma = \sum_\omega S(k, \omega) \ln[S(k, \omega)/m(\omega)]$. We have used a flat default model $m(\omega)$, which is iteratively adjusted to match the zeroth moment of the trial spectrum. The optimal spectrum follows from the average of $S(k, \omega)$, weighted by a probability distribution $P[\alpha|S(k, \omega)]$ (see [33]).

IV. RESULTS

In this section, we will detail our results for the finite temperature susceptibility and the dynamic structure factor. For the former we will contrast perturbation theory (PT) with QMC. One of the quantities of prime interest to be extracted from this is the spin gap, which we will discuss also.

A. Magnetic susceptibility

Perturbation theory (PT): For $j \ll 1$ we first consider the coupling between the AF dimers perturbatively. Following Ref. [35], we expand to $O(j^1)$. This turns the problem into a *tight-binding* model for a gas of *non-interacting* triplets with nearest-neighbor hopping along the chain (triplons) which acquire a dispersion of

$$\epsilon_k = J_{\text{AF}} - \frac{J_{\text{F}}}{2} \cos(ka) = \Delta - \frac{J_{\text{F}}}{2} (1 + \cos(ka)), \quad (6)$$

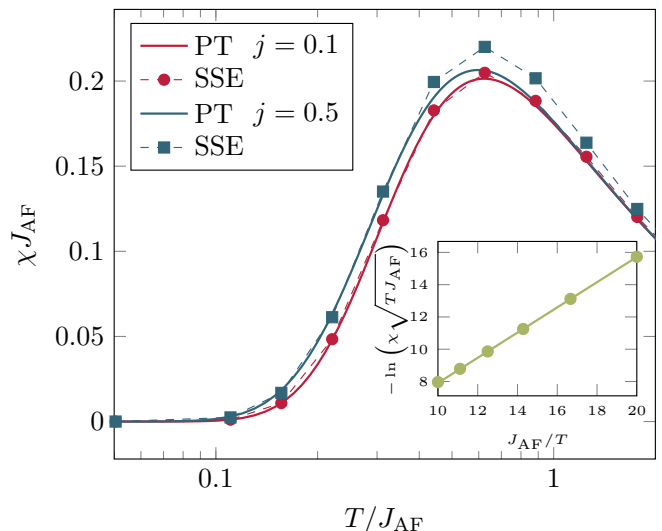


FIG. 2: Susceptibility versus T for $j=0.1$ and 0.5 obtained from PT (solid) and SSE (dashed with markers). For SSE the error is less than the marker size. Inset: Typical fits of Eq. (11) (solid) to SSE (markers) in the low- T range for $j = 2$, where the gap Δ can be extracted from the slope.

where the length of the unit cell $a \equiv 2$ is set out hereafter. $\Delta = \epsilon_{\pi/a} = J_{\text{AF}} + \frac{J_{\text{F}}}{2}$ is the gap. The free energy of such triplon gases is given by [36]

$$f = -\frac{1}{2\beta} \ln \left\{ 1 + [1 + 2 \cosh(\beta h)] \sum_k e^{-\beta \epsilon_k} \right\}. \quad (7)$$

The momentum summation $z(\beta) = \sum_k e^{-\beta \epsilon_k}$ can be evaluated as

$$z(\beta) = \frac{1}{2\pi} \int_{-\pi}^{\pi} dk e^{-\beta \epsilon_k} = e^{\beta J_{\text{AF}}} I_0 \left(\frac{\beta J_{\text{F}}}{2} \right), \quad (8)$$

where $I_0(x) = \sum_n (x^2/4)^n / (n!)^2$ is the modified Bessel function of the first kind [37]. From this the susceptibility can be obtained analytically by

$$\chi(T) = -\frac{\partial f}{\partial h^2} \Big|_{h=0} = \beta \frac{z(\beta)}{1 + 3z(\beta)}. \quad (9)$$

SSE quantum Monte Carlo: The susceptibility can be calculated within the SSE method by measuring the sum over the spin configurations

$$\chi = \frac{1}{T} \left(\left\langle \left(\sum_i S_i^z \right)^2 \right\rangle - \left\langle \sum_i S_i^z \right\rangle^2 \right). \quad (10)$$

For low temperatures the energy gap between the ground state and the first excited state can be extracted according to [38]

$$\chi(T) \propto \sqrt{\beta} e^{-\beta \Delta}, \quad (11)$$

which stems from the asymptotic expansion of the modified Bessel function for large arguments [37] in Eq. (9).

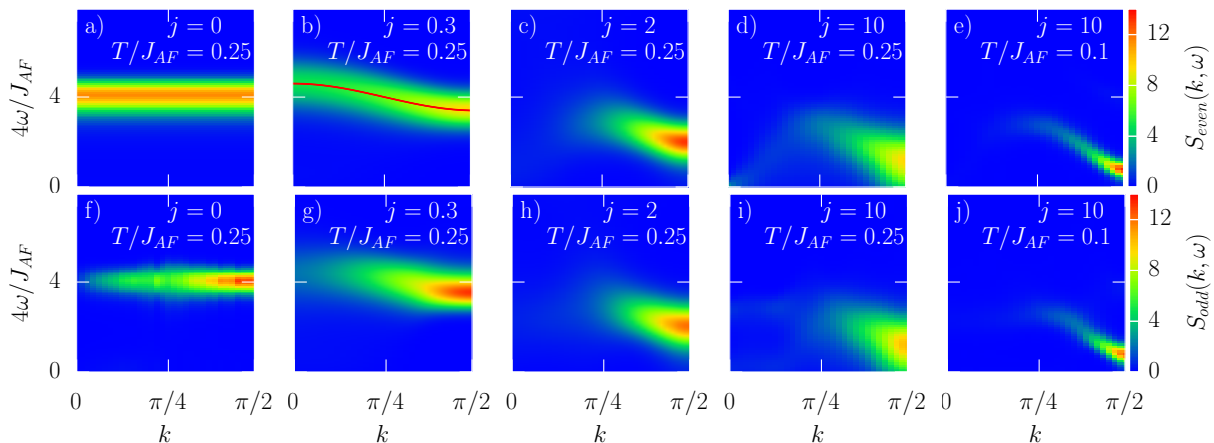


FIG. 3: Contour maps of the dynamic structure factors $S_{even/odd}(k, \omega)$ for various $j=0, 0.3, 2$, and 10 , as well as for temperatures $T/J_{AF}=0.25$ and 0.1 on a FAC with $N = 128$ sites. Solid line in panel b) refers to PT, Eq. (6). Color coding of intensity (bar on rightmost panels) identical in all plots.

Fig. 2 shows $\chi(T)$ for a low and an intermediate temperature range and for small, as well as for intermediate $j=0.1$ and 0.5 , respectively. As is obvious PT and SSE agree very well for $T/J_{AF} \ll 1$ and for both values of j . Interestingly, this agreement holds up to $j=0.5$ even at intermediate T/J_{AF} , where only a $\sim 10\%$ difference can be observed at the correlation maximum. Because of the excellent agreement at low T/J_{AF} , fitting the SSE with Eq. (11) is well justified. We note in passing that for $T/J_{AF} \gg 1$, PT and SSE both approach Curie behavior, with $\chi(T) = C_c/T$, and a Curie constant $C_c = 1/4$ per spin.

B. Dynamic structure factor

Now we turn to the finite-temperature dynamic structure factor. Fig. 3 displays contour maps of $S_{even/odd}(k, \omega)$ over a wide range of j -values and for two temperatures. The figure conveys four main messages.

First, there is an obvious evolution of dispersive behavior starting with a k -independent gap at $j=0$. The latter simply reflects the spectrum of the exact AF-dimer product-state, which comprises delta-functions at the singlet-triplet gap $\omega = J_{AF}$. Increasing j , one remains within the range of validity of PT, where we expect $S_{even/odd}(k, \omega)$ to encode a cosine-band of dispersing triplets. As is shown in Fig. 3b) the center of gravity of the spectrum fits perfectly to Eq. (6) indeed. Finally, as j is increased further, the system crosses over into a correlated state displaying a small but *finite* gap at which the Brillouin zone (BZ) boundary intensity is maximal. We find, that increasing j beyond the value of $j^* \sim O(10)$, has little effect on the size of this gap. We conclude, that $j > j^*$ is the regime of the effective Haldane chain.

Second, Fig. 3 displays a gradual redistribution of spectral weight for S_{even} with increasing j , starting from a situation with significant intensity extending over all of

the BZ at $j \ll 1$, to a prominent modulation of the spectral weight located at the zone boundary, occurring for $j \gg 1$. This is a direct manifestation of the increase of the AF spin-correlation length ξ versus j as the Haldane limit is approached. In fact for $j = 0$, AF correlations extend only over a single dimer, while in the Haldane limit $\xi \simeq 6$, referring to $S=1$ -sites [27], i.e. FM dimers in our case. This increase of ξ translates into a static structure factor $S_k \sim \int_0^\infty d\omega S(k, \omega)$, which evolves from a momentum independent function at $j=0$ to one which displays an increase as $k \rightarrow \pi/2$ for $j \rightarrow \infty$. This causes the intensity modulation, observable in $S_{even}(k, \omega)$. For S_{odd} , already at $j \ll 1$ the spectral weight is located at the zone boundary because of an additional trivial modulation by on-dimer correlations as described in Eq. (4).

Third, there is a clear thermal broadening of the spectra as T increases. This can be seen in Fig. 3d), e) and i), j) at $j=10$. In both cases the $T=0.1$ spectra are rather sharp. They display a clear gap even for $j=10$ and very much resemble that of the Haldane chain at $T = 0$ [27, 39–42]. Increasing T/J_{AF} to 0.25 , keeping j fixed, the spectra are broadened and the gap is practically closed. Again this is similar to finite temperature analysis of the pure Haldane chain [41–43].

Fourth, there is only a small difference between $S_{even/odd}(k, \omega)$ in an intensity modulation along k . As described in Eq. (4), the on-site/bond correlators are included and are leading to this difference clearly seen for $j = 0$.

Out of scale of Fig. 3 is another band at the ferromagnetic dimer $\omega = j$ with low intensity. Only for $j \geq 2$ this band is well separated from the dispersive band. In MEM therefore, the whole spectrum and thus a larger ω -regime must be considered.

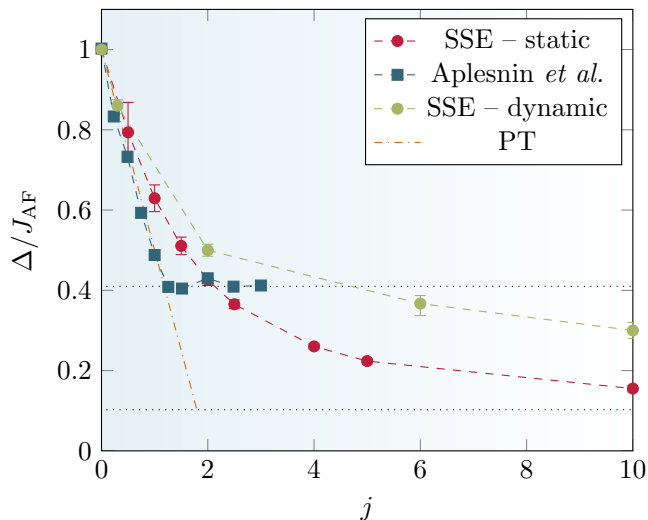


FIG. 4: Spin gap versus j , obtained from various methods: PT, thermodynamic and dynamic QMC. Dotted horizontal lines: conventional Haldane gap ≈ 0.41 and one fourth thereof. For dynamic QMC the error is the full width at half maximum.

C. Gap evolution

In this subsection we summarize our findings for the spin gap versus j . To this end, in Fig. 4, we have collected Δ/J_{AF} as obtained from our PT, thermodynamic SSE, and dynamic SSE calculations. For dynamic SSE, the gap is defined by the energy ω_{max}/J_{AF} at the maximum of $S(k, \omega)$ at $k = \pi/2$. In addition, the figure also contains QMC data from Aplesnin and Petrakovskii [12].

First, it is obvious, that for $j \lesssim 1$ all methods result in a gap of comparable magnitude, which decreases rapidly with j . Second, for $j \gtrsim 1$ PT underestimates the gap size. Third, thermodynamic and dynamic SSE both show the same trend of the gap, i.e. to converge to a value which is clearly less than the single spin-1 Haldane chain. For Δ as from thermodynamic SSE and Eq. (11) is tempting to speculate, that indeed $\Delta(j \rightarrow \infty) = \Delta_H/4$ as conjectured in Section II. The gap from dynamic SSE shows a similar trend, however the convergence to the anticipated

value of $\Delta_H/4$ is significantly slower. Since $\chi(T)$ rather refers to a measure of an integrated density of states, than a peak position, a *quantitative* difference in Δ as obtained from thermodynamic and dynamic QMC is not surprising. Turning to Ref. [12], where the gap has also been extracted from fits to $\chi(T)$, obtained by a QMC method, we note that agreement with our results is visible for $\Delta \geq \Delta_H$, i.e. for $j \lesssim 1$. However beyond that, Δ from Ref. [12] is pinned to Δ_H . This is a variance not only with our results, but also with Ref. [28]. The cause of this remains unclear at present.

V. CONCLUSION

To summarize, we have studied static and dynamic properties of alternating ferro-antiferromagnetic spin-1/2 chains at finite temperature. We observe a smooth crossover from weakly coupled dimer to Haldane-chain behavior versus j with *no* intervening quantum critical point. Both, thermodynamic and dynamic QMC suggest that lowest-order PT for a dispersive triplon gas describes the physics well up to $j \sim 1$. At $j \gtrsim 10$ effective Haldane physics emerges, with an asymptotic spin gap reduced by a factor of 4 as compared to the conventional Haldane gap. Because of the latter reduction, the impact of finite temperature is significant already a $T/J_{AF} \gtrsim 0.25$, where we find the gap to be filled in completely.

While we have focused on periodic boundary conditions, open chains can equally well be studied by SSE QMC. This would allow to analyze the fate of topological edge states versus j and temperature. In view of the existing materials, $C_{29}H_{18}F_{12}N_5O_4Zn$ [13] and $BaCu_2V_2O_8$ [24], more realistic dynamic QMC calculations, including inter chain exchange should be an additional direction of future research.

Acknowledgments

This work has partially been supported by the State of Lower Saxony through QUANOMET (project NP-2) and by the DFG via SFB 1143 (Project A02). W. B. acknowledges kind hospitality of the PSM, Dresden.

[1] F. D. M. Haldane, Phys. Lett. A **93**, 464 (1983).
[2] M. den Nijs and K. Rommelse, Phys. Rev. B **40**, 4709 (1989).
[3] H. Tasaki, Phys. Rev. Lett. **66**, 798 (1991).
[4] I. Affleck, T. Kennedy, E. H. Lieb, H. Tasaki, Phys. Rev. Lett. **59**, 799 (1987).
[5] J. J. Borrás-Almenar, E. Coronado, J. Curely, R. Georges, and J. C. Gianduzzo, Inorganic Chemistry **33**, 5171 (1994).
[6] S. Watanabe and H. Yokoyama, J. Phys. Soc. Jpn. **68**, 2073 (1999).
[7] K. Hida, Phys. Rev. B **45**, 2207 (1992).

[8] T. Sakai, J. Phys. Soc. Jpn. **64**, 251 (1995).
[9] S. Kokado and N. Suzuki, J. Phys. Soc. Jpn. **68**, 3091 (1999).
[10] S. Paul and A. K. Ghosh, Condensed Matter Physics **20**, 23701 (2017).
[11] Y.-Z. Wu and Z.-Y. Li, Physica Status Solidi (B) **213**, 27 (1999).
[12] S. S. Aplesnin and G. A. Petrakovskii, Phys. Solid State **41**, 1511 (1999).
[13] H. Yamaguchi, Y. Shinpuku, T. Shimokawa, K. Iwase, T. Ono, Y. Kono, S. Kittaka, T. Sakakibara, and Y. Hosokoshi, Phys. Rev. B **91**, 085117 (2015).

- [14] M. Hagiwara, Y. Narumi, K. Kindo, T. C. Kobayashi, H. Yamakage, K. Amaya, and G. Schumauch, *J. Phys. Soc. Jpn.* **66**, 1792 (1997).
- [15] Y. Hosokoshi, Y. Nakazawa, K. Inoue, K. Takizawa, H. Nakano, M. Takahashi, and T. Goto, *Phys. Rev. B* **60**, 12924 (1999).
- [16] K. Kodama, H. Harashina, H. Sasaki, M. Kato, M. Sato, K. Kakurai, and M. Nishi, *J. Phys. Soc. Jpn.* **68**, 237 (1999).
- [17] Y. Inagaki, Y. Sakamoto, H. Morodomi, T. Kawae, Y. Yoshida, T. Asano, K. Hosoi, H. Kobayashi, H. Kitagawa, Y. Ajiro, and Y. Furukawa, *J. Phys. Soc. Jpn.* **83**, 054716 (2014).
- [18] K. Kodama, T. Fukamachi, H. Harashina, M. Kanada, Y. Kobayashi, M. Kasai, H. Sasai, M. Sato, and K. Kakurai, *J. Phys. Soc. Jpn.* **67**, 57 (1998).
- [19] Y. Ajiro, K. Takeo, Y. Inagaki, T. Asano, A. Shimogai, M. Mito, T. Kawae, K. Takeda, T. Sakon, H. Nojiri, and M. Motokawa, *Physica B* **329-333**, 1008 (2003).
- [20] M. B. Stone, W. Tian, M. D. Lumsden, G. E. Granroth, D. Mandrus, J.-H. Chung, N. Harrison, and S. E. Nagler, *Phys. Rev. Lett.* **99**, 087204 (2007).
- [21] Y. Miura, R. Hirai, Y. Kobayashi, and M. Sato, *J. Phys. Soc. Jpn.* **75**, 084707 (2006).
- [22] Y. Miura, Y. Yasui, T. Moyoshi, M. Sato, and K. Kakurai, *J. Phys. Soc. Jpn.* **77**, 104709 (2008).
- [23] C. N. Kuo, T. S. Jian, and C. S. Lue, *J. Alloys Compd.* **531**, 1 (2012).
- [24] E. S. Klyushina, A. T. M. N. Islam, J. T. Park, E. A. Goremychkin, E. Wheeler, B. Klemke, and B. Lake, *Phys. Rev. B* **98**, 104413 (2018).
- [25] R. Botet and R. Jullien, *Phys. Rev. B* **27**, 613 (1983).
- [26] M. P. Nightingale and H. W. J. Blte, *Phys. Rev. B* **33**, 659 (1986).
- [27] S. R. White and D. A. Huse, *Phys. Rev. B* **48**, 3844 (1993).
- [28] H.-H. Hung and C.-D. Gong, *Phys. Rev. B* **71**, 054413 (2005).
- [29] B. Bauer, L. D. Carr, H. G. Evertz, *et al.*, *J. Stat. Mech.* P05001 (2011).
- [30] A. W. Sandvik, *J. Phys. A* **25**, 3667 (1992).
- [31] A. W. Sandvik, *Phys. Rev. B* **59**, R14157 (1999).
- [32] O. F. Syljuåsen and A. W. Sandvik, *Phys. Rev. E* **66**, 046701 (2002).
- [33] J. Skilling and R. K. Bryan, *Mon. Not. R. Astron. Soc.* **211**, 111 (1984).
- [34] M. Jarrell and J. Gubernatis, *Phys. Rep.* **269**, 133 (1996).
- [35] A. J. A. James, F. H. L. Essler, and R. M. Konik, *Phys. Rev. B* **78**, 094411 (2008).
- [36] M. Troyer, H. Tsunetsugu, and D. Würtz, *Phys. Rev. B* **50**, 13515 (1994).
- [37] M. Abramowitz, *Handbook of mathematical functions: with formulas, graphs, and mathematical tables* (Dover Publications, New York, 1970).
- [38] K. Damle and S. Sachdev, *Phys. Rev. B* **57**, 8307 (1998).
- [39] M. Takahashi, *Phys. Rev. Lett.* **62**, 2313 (1989).
- [40] O. Golinelli, T. Jolicoeur, and R. Lacaze, *J. Phys.: Condens. Matter* **5**, 1399 (1993).
- [41] S. N. Grossjohann, *Static and Dynamic Properties of Low Dimensional Quantum Spin Systems*, dissertation, Technische Universität Braunschweig, Cuvillier Verlag Göttingen, 2010.
- [42] Y. Rahnavard and W. Brenig, *Phys. Rev. B* **91**, 054405 (2015).
- [43] J. Richter, N. Casper, W. Brenig and R. Steinigeweg, *Phys. Rev. B* **100**, 144423 (2019).